

PEG-based passivation and functionalization of diamond surfaces for biomolecular quantum sensing

Ziting Sun^{1,2}, Sanyou Chen^{1,2,3,4} ✉, Wanhe Li^{1,2,3,4}, Shijie Li^{1,2,3,4}, and Fazhan Shi^{1,2,3,4,5} ✉

¹Laboratory of Spin Magnetic Resonance, School of Physical Sciences, University of Science and Technology of China, Hefei 230026, China;

²Anhui Province Key Laboratory of Scientific Instrument Development and Application, University of Science and Technology of China, Hefei 230026, China;

³School of Biomedical Engineering, University of Science and Technology of China, Hefei 230026, China;

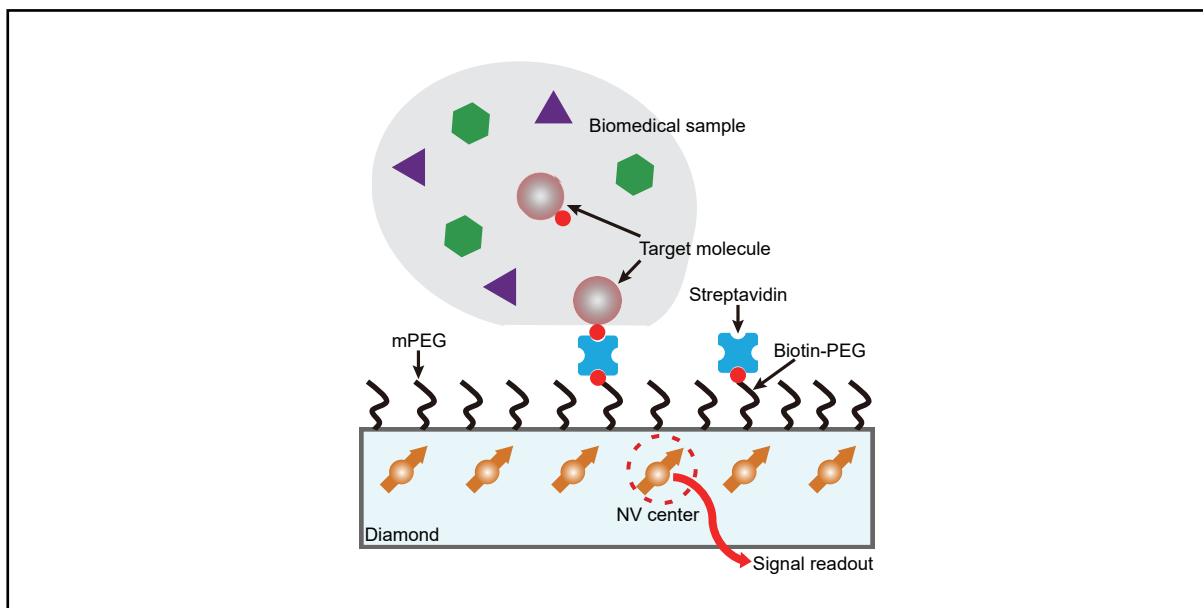
⁴Suzhou Institute for Advanced Research, University of Science and Technology of China, Suzhou 215123, China;

⁵Hefei National Laboratory, University of Science and Technology of China, Hefei 230088, China

✉ Correspondence: Sanyou Chen, E-mail: sanyou@ustc.edu.cn; Fazhan Shi, E-mail: fzshi@ustc.edu.cn

© 2025 The Author(s). This is an open access article under the CC BY-NC-ND 4.0 license (<http://creativecommons.org/licenses/by-nc-nd/4.0/>).

Graphical abstract



PEG-based passivation and functionalization of the diamond surface enable practical and specific nitrogen–vacancy center-based quantum sensing of biomolecules.

Public summary

- We systematically tailor and optimize polyethylene glycol (PEG)-based treatments for diamond surfaces to establish a standardized method that effectively reduces nonspecific binding (NSB) while producing sufficient specific binding sites for nitrogen–vacancy (NV)-based biomolecular quantum sensing.
- Our results showed that either a mixture of 5 kDa PEG and biotin-PEG in a $\geq 5 : 1$ ratio (PEG to biotin-PEG) or 20 kDa biotin-PEG alone achieved an optimal balance between NSB suppression and efficient specific binding of biomolecules and nanoparticles.
- The PEGylation process preserved the magnetic-sensing properties of NV centers, and we validated the method via an immunomagnetic assay of antibodies in human serum samples.

PEG-based passivation and functionalization of diamond surfaces for biomolecular quantum sensing

Ziting Sun^{1,2}, Sanyou Chen^{1,2,3,4} ✉, Wanhe Li^{1,2,3,4}, Shijie Li^{1,2,3,4}, and Fazhan Shi^{1,2,3,4,5} ✉

¹Laboratory of Spin Magnetic Resonance, School of Physical Sciences, University of Science and Technology of China, Hefei 230026, China;

²Anhui Province Key Laboratory of Scientific Instrument Development and Application, University of Science and Technology of China, Hefei 230026, China;

³School of Biomedical Engineering, University of Science and Technology of China, Hefei 230026, China;

⁴Suzhou Institute for Advanced Research, University of Science and Technology of China, Suzhou 215123, China;

⁵Hefei National Laboratory, University of Science and Technology of China, Hefei 230088, China

✉ Correspondence: Sanyou Chen, E-mail: sanyou@ustc.edu.cn; Fazhan Shi, E-mail: fzshi@ustc.edu.cn

© 2025 The Author(s). This is an open access article under the CC BY-NC-ND 4.0 license (<http://creativecommons.org/licenses/by-nc-nd/4.0/>).



Cite This: *JUSTC*, 2025, 55(10): 1002 (8pp)



Read Online

Abstract: The reduction of nonspecific binding (NSB, or passivation) and functionalization of the diamond surface are crucial for nitrogen-vacancy (NV) center-based quantum sensing in biomedical systems, especially for biomolecular detection. In this work, we systematically investigated polyethylene glycol (PEG)-based treatment technologies for the passivation and functionalization of diamond surfaces. Specifically, we evaluated the passivation and functionalization effects of PEG with different chain lengths and then the impact of streptavidin proteins on these treatments. Our results show that either a mixture of 5 kDa PEG and biotin-PEG in a $\geq 5 : 1$ ratio (PEG to biotin-PEG) or 20 kDa biotin-PEG alone coordinated the suppression of NSB and efficient specific binding of biomolecules and nanoparticles. In addition, we confirmed that the magnetic-sensing-related properties of NV centers were not affected by the PEGylation process and verified the applicability of our diamond treatment scheme with an immunomagnetic assay of antibodies in human serum samples. Overall, our study provides an effective biocompatible treatment strategy and practical protocols for diamond surfaces, promoting NV center-based quantum sensing of biomolecules.

Keywords: diamond surface; PEGylation; nonspecific binding; functionalization; quantum sensing

CLC number: O59

Document code: A

1 Introduction

The nitrogen-vacancy (NV) center in diamond is a promising sensitive quantum sensor for magnetism, temperature, and electric charge^[1]. Recent advances have expanded its applications in biomedical fields^[2,3], including the detection of single molecules^[4–6], single cells^[7,8], tumor tissues^[9], and physiological processes^[10]. Among them, NV center-based biomolecular detections are impressive, such as detecting single-molecule nuclear magnetic resonance (NMR) and electron paramagnetic resonance (EPR) spectroscopy^[4–6] and biomolecular interactions^[11], and highly sensitive assays of biomolecules^[12,13]. In these detections, which are limited by the detection region of NV centers, analytes should be prepared on or near the diamond surface. However, nonspecific binding (NSB) at the surface compromises the detection specificity and sensitivity—a pervasive challenge for interface-based sensing technologies^[14–16]. Therefore, it is critical to develop treatment techniques for diamond surfaces to minimize NSB and promote specific binding of biomolecules.

Prior to the advent of NV center-based quantum sensing, diamond surface treatment for traditional applications relied mainly on hydrogen termination via high-temperature plasma processes^[17], followed by electrochemical^[18,19] or photochemical^[18,20,21]

functionalization. However, these hydrogenation methods severely degrade NV center performance by diminishing the fluorescence intensity or even eliminating detectable emission^[22–24], concurrently increasing the degree of technical complexity. For diamond quantum sensing, recent advancements employing ammonia plasma^[25], atomic layer deposition (ALD)^[26], and optimized photochemical techniques^[27] have attempted to address the above issues. Unfortunately, these treatments face critical trade-offs. For instance, for single-molecule detection, the ALD layer adds to the spatial separation between NV centers and target molecules while reducing NV coherence times^[26]. Most importantly, most of the above efforts prioritize maximizing molecule-binding efficiency, ignoring the need to minimize background signals from nonspecific interactions—a barrier that fundamentally limits sensor specificity in complex environments.

Polyethylene glycol (PEG) is a biocompatible and versatile polymer widely used in various biomedical fields, such as molecular studies, functional biomaterials, and drug delivery^[28]. In single-molecule studies, PEG/biotin-PEG is usually used to passivate detection interfaces and prepare single-molecule samples^[29–31], suggesting that PEG is a potentially suitable material for diamond treatments. In our previous work, we utilized PEG to treat the diamond surface for

magnetic detection of biomolecular interactions^[1]. However, a comprehensive investigation of PEG-based modification techniques for diamond surfaces has not yet been conducted.

In this work, we systematically tailor and optimize PEG treatments to establish a standardized method that suppresses NSB while providing appropriate specific binding sites on diamonds, enabling practical NV-based biomolecular quantum sensing. Our results show that, on diamonds, generally, 5–20 kDa PEG (PEG/biotin-PEG) can fulfill the requirements of minimizing NSB and specific binding. However, streptavidin (SA) binding to 5 kDa biotin-PEG severely disrupted NSB suppression, which was mitigated by using 20 kDa biotin-PEG or a 5 kDa PEG mixture with a $\geq 5 : 1$ ratio of PEG to biotin-PEG. Finally, the basic properties of NV sensors are not affected by PEGylation, and we specifically examined SARS-CoV-2-induced antibodies in the serum of a convalescent patient with COVID-19.

2 Materials and methods

2.1 Diamond sensors

The diamonds with or without NV centers used in this work were prepared and described in our previous work^[1]. In brief, the bulk diamonds grown via chemical vapor deposition (CVD) were purchased from Element Six. These electronic-grade [100] diamonds were 2 mm \times 2 mm \times 0.5 mm in size. In NV-property measurements and single-particle magnetic imaging, NV-containing diamonds have an NV ensemble layer with an NV density of $\sim 1.7 \times 10^{11}$ cm⁻² and a depth of ~ 20 nm.

2.2 PEG treatments of diamond surfaces

First, the diamonds were soaked in freshly prepared piranha solution (H₂SO₄ : H₂O₂ = 3 : 1 v/v) at 180 °C for 2 h. After treatment, they were thoroughly rinsed with deionized water and methanol. (3-aminopropyl)triethoxysilane (APTES, Sigma–Aldrich, 440140) was then added to the diamonds, which were subsequently incubated at room temperature for 1 h. The aminated diamonds were rinsed three times with methanol and five times with deionized water.

For PEG-based passivation and functionalization of diamond surfaces, methyl-terminated NHS (N-hydroxysuccinimide)-ester PEG with a molecular weight (MW) of 550 Da, 1 kDa, 2 kDa, 5 kDa, 10 kDa, or 30 kDa (mPEG; Shanghai Pengsheng Biological or Laysan Bio. Inc.), biotinylated NHS (N-hydroxysuccinimide)-ester PEG with a (MW) of 2 kDa, 5 kDa, 10 kDa, or 20 kDa (biotin-PEG; Shanghai Pengsheng Biological or Laysan Bio. Inc.), and a mixture of mPEG and biotin-PEG with a given ratio were used. For the treatment effect of different chain lengths, PEGs were purchased from Shanghai Pengsheng Bio. For the effect of streptavidin and biomolecular detection experiments, PEGs were purchased from Laysan Bio. The PEG solution (~ 200 mg/mL in 0.1 M NaHCO₃, pH 8.3) was prepared and immediately added to the diamonds. The reaction systems were placed in a light-shielded humidified box and incubated for 3 h at room temperature or overnight at 4 °C. To increase the passivation efficiency, the PEG treatment can be repeated. After the reaction, the PEGylated diamonds were rinsed five times with water.

2.3 Preparation of biomolecules and magnetic nanoparticles on diamonds

For streptavidin (SA) impact evaluation and receptor-binding domain (RBD) antibody detection, SA (0.6 mg/mL, Sigma–Aldrich, S0677) was preimmobilized on biotin-PEG-functionalized diamonds by incubating for 30 min. Biotinylated RBD proteins (0.1 mg/mL, Sino Biological, 40592-V08B-B) were then added to SA-modified diamonds and incubated for an additional 30 min. To evaluate nonspecific binding (NSB) and molecular binding efficiency on PEG-modified diamonds, 1–2 μ L of BSA-TRITC (~ 1 mg/mL, Xi'an RuiXi Biotechnology) or Alexa Fluor 488 (AF488)-labeled SA-MNPs (4 pM) were added onto the diamond surface and incubated for 1 h. To assess the impact of SA, 1–2 μ L of AF488-labeled IgG-MNPs was incubated on SA-modified diamonds for 30 min. For spike-RBD antibody detection, RBD-modified diamonds were incubated with blood samples, approved by the Ethics Committee of the First Affiliated Hospital of USTC (2023-KY (H)-006), for 30 min. Then, AF488-IgG-MNPs (4 pM) were added and incubated for 15 min. The MNP conjugation followed our prior protocols^[1]. All the diamonds were rinsed with PBS before imaging.

2.4 Fluorescence imaging

To balance experimental efficiency with practical applicability, passivation and functionalization effects were assessed via wide-field fluorescence imaging. The fluorescence imaging was mainly performed in an inverted fluorescence microscope (Olympus IX73), which was equipped with an EMCCD camera (Andor, iXon Ultra 897) and an oil-immersion objective (Olympus; PLAPON 60 \times , numerical aperture (NA) 1.42). The exposure times ranged from 0.1 to 0.5 s. Other imaging was performed in an upright microscope (Olympus BX53) with an sCMOS camera (Andor, Neo5.5) and a 100 \times objective (Olympus MPLFLN 100 \times , NA 0.9).

2.5 Single-particle immunomagnetic assay of anti-spike RBD antibodies

Single-particle magnetic imaging was performed in our custom-built diamond magnetic microscope^[1]. In brief, we mapped the magnetic field by acquiring the continuous-wave (CW) spectrum of NV centers. The microwave frequencies were swept (1 MHz step, 25 MHz range) across $|0\rangle \rightarrow |-1\rangle$ and $|0\rangle \rightarrow |+1\rangle$ transitions, with fluorescence captured via sCMOS (0.1 s exposure). A 50-sweep average ensured a high signal-to-noise ratio (SNR). Spectral fitting and baseline detrending were performed via our custom-built program in MATLAB R2018b.

2.6 Statistical analysis

The fluorescence intensity and MNP count were analyzed in ImageJ and a custom MATLAB program^[32], respectively. The data presented in the histograms are expressed as the mean value \pm standard error of the mean (SEM). Two-sample *t* tests and statistical analyses were performed in Origin 2020.

3 Results and discussion

3.1 Basic procedures of PEG-based passivation and functionalization

The workflow of PEG-based passivation and functionalization

of the diamond surface is shown in Fig. 1 (see Section 2 for detailed procedures). First, the bare bulk diamond is soaked in piranha solution to generate a surface with hydroxyl groups. Then, (3-aminopropyl)triethoxysilane (APTES) is added to form an aminated surface. After that, PEG is immobilized on the surface via the covalent reaction of amino and carboxyl groups (NHS is used as the activated carboxyl group). This process, also known as surface passivation, eliminates NSB on the diamond surface by introducing PEG/biotin-PEG molecules. In our experiments, methoxy-terminated PEG (mPEG) was used as the normal PEG, and biotin terminated PEG (biotin-PEG) was used as the functionalized PEG. By adjusting the ratio of mPEG to biotin-PEG, we can also control the density or average spacing of binding sites at the interface. Subsequently, streptavidin (SA) binds to the surface via the biotin-SA interaction. Finally, biomolecules are captured on the SA-coated diamond for molecular-level quantum sensing. The diamond can easily be cleaned and recycled in piranha solution. As an alternative way for hydroxylation^[30], the alkali solution treatment was less efficient at generating hydroxyl groups and eliminating NSB on the diamond surface (Fig. S1 in Supporting information).

3.2 The chain length of PEG determines the treatment effect on the diamond surface

The chain length of PEG usually affects the results of both surface passivation and functionalization^[33]. As shown in our previous study, there were also obvious NSBs of various proteins on the bare diamonds^[11]. Here, we evaluated the effectiveness of mPEG with different MWs in eliminating NSB on the diamonds by examining fluorescent bovine serum albumin (BSA-TRITC). The chain length and physical size of PEG are proportional to its MW. To match the polymer dimension with the surface coverage on the diamonds and referring to studies on glass substrates^[33–35], we selected 550 Da to 30 kDa PEGs for the diamond experiments. As shown in Fig. 2, NSB was obvious on the surface of the low-MW (550 Da) mPEG-treated diamond. As the PEG weight increased to 2 kDa or greater, the NSB was significantly reduced. Notably,

surface modification with 10 kDa mPEG presented the lowest level of NSB. However, with further increases in the MW, such as 30 kDa, NSB resurgence was observed. Overall, mPEGs with different chain lengths have distinct passivation effects on diamonds. Among them, PEG, with MWs ranging from 2 kDa to 30 kDa, can significantly inhibit NSB (Fig. 2b and c). As a contrast, on glass substrates, 5 kDa PEG achieves an optimal balance between moderate chain length (providing adequate thickness for steric repulsion) and sufficient packing density (minimizing interchain gaps), thereby enhancing both steric and hydration barriers^[33]. The results for the diamond surfaces followed a similar MW-dependent trend, with slightly different optimal MW (10 kDa PEG) for NSB suppression (Fig. 2). We explain here that our supplier lacks 20 kDa mPEG and 30 kDa biotin-PEG related to the following experiments in the next paragraph.

Biotin-PEG serves not only as a tool for eliminating NSB but also as an anchor for biomolecule binding at the detection interface. To evaluate the efficiency of molecule or nanoparticle binding, we applied streptavidin (SA)-coated magnetic nanoparticles (MNPs) with the fluorescent label Alexa Fluor 488 (AF488-SA-MNP) to diamond surfaces treated with biotin-PEG with various MWs. The single-particle fluorescence images indicated that, on the diamonds coated by biotin-PEG with MWs of 2 kDa, 5 kDa, 10 kDa, or 20 kDa, there were the fewest MNPs in the 2 kDa group and the most MNPs in the 5 kDa group (Fig. 3). Consequently, 5 kDa biotin-PEG was determined to be the most suitable for functionalizing diamond surfaces in terms of biomolecule binding efficiency. Considering the two factors of eliminating NSB and increasing the molecule binding efficiency, we conclude that each of 5 kDa, 10 kDa, and 20 kDa PEG (mPEG/biotin-PEG) is able to achieve a good modification effect on the diamond surface.

3.3 Impact of streptavidin binding on surface modification

The biotin-streptavidin (SA) system usually serves as a molecular bridge at the detection interface^[36]. For instance, in

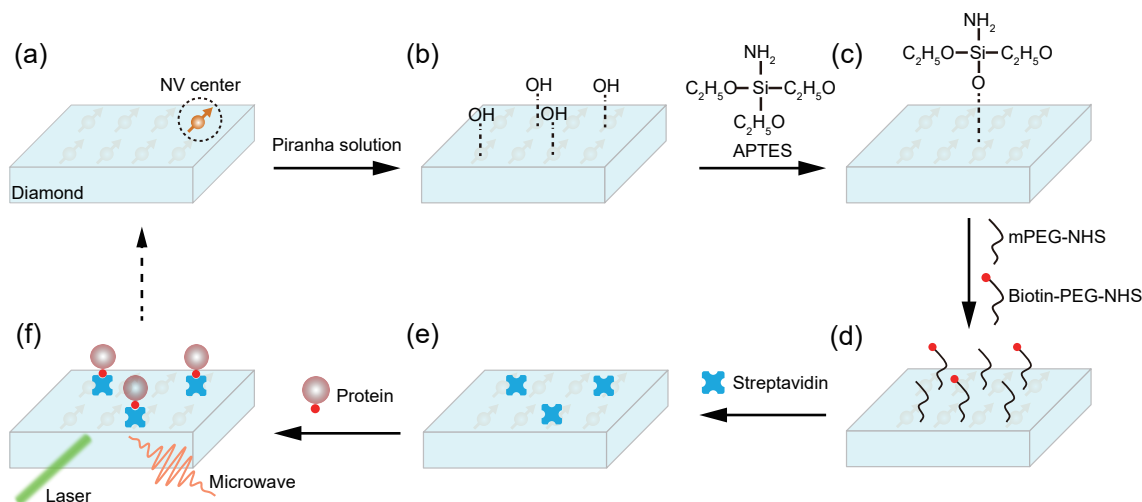


Fig. 1. Workflow of polyethylene glycol (PEG)-based passivation and functionalization of a diamond surface. (a) Bare diamond. A shallowly embedded NV layer is present in the diamond. (b) Hydroxyl-terminated diamond after piranha solution treatment. (c) Aminated terminated diamond after APTES treatment. (d) PEGylated diamond. (e) Diamond with immobilized streptavidin. (f) Biomolecules on diamond for quantum sensing.

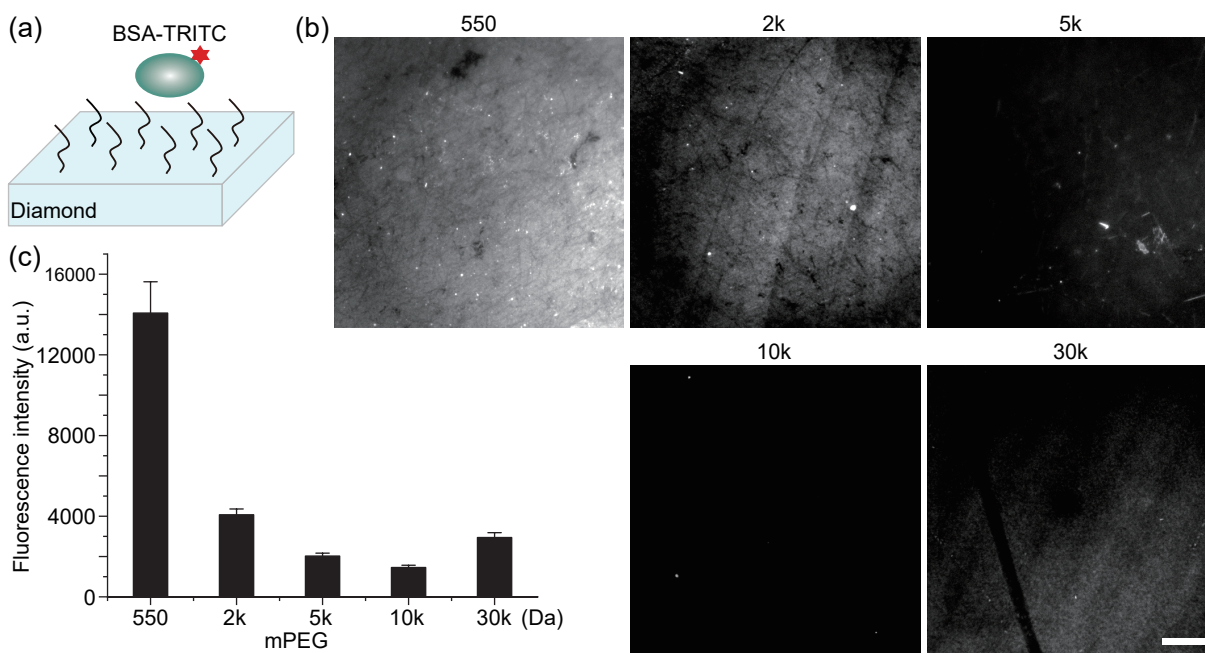


Fig. 2. PEGs with different molecular weights have different efficiencies for eliminating NSB on the diamond surface. (a) Schematic of the NSB examination. BSA-TRITC was employed to evaluate the extent of NSB. (b) Fluorescence images of BSA-TRITC on diamonds treated with 100% mPEG with different MWs. The MWs of mPEG are indicated in the figure. The PEGs were used at the same excess concentration of 200 mg/mL in all the experiments in this work. Scale bar, 20 μm . (c) Quantification of the fluorescence intensities in (b). Data are presented as the mean \pm standard error of the mean (SEM), $n \geq 10$ areas for each group.

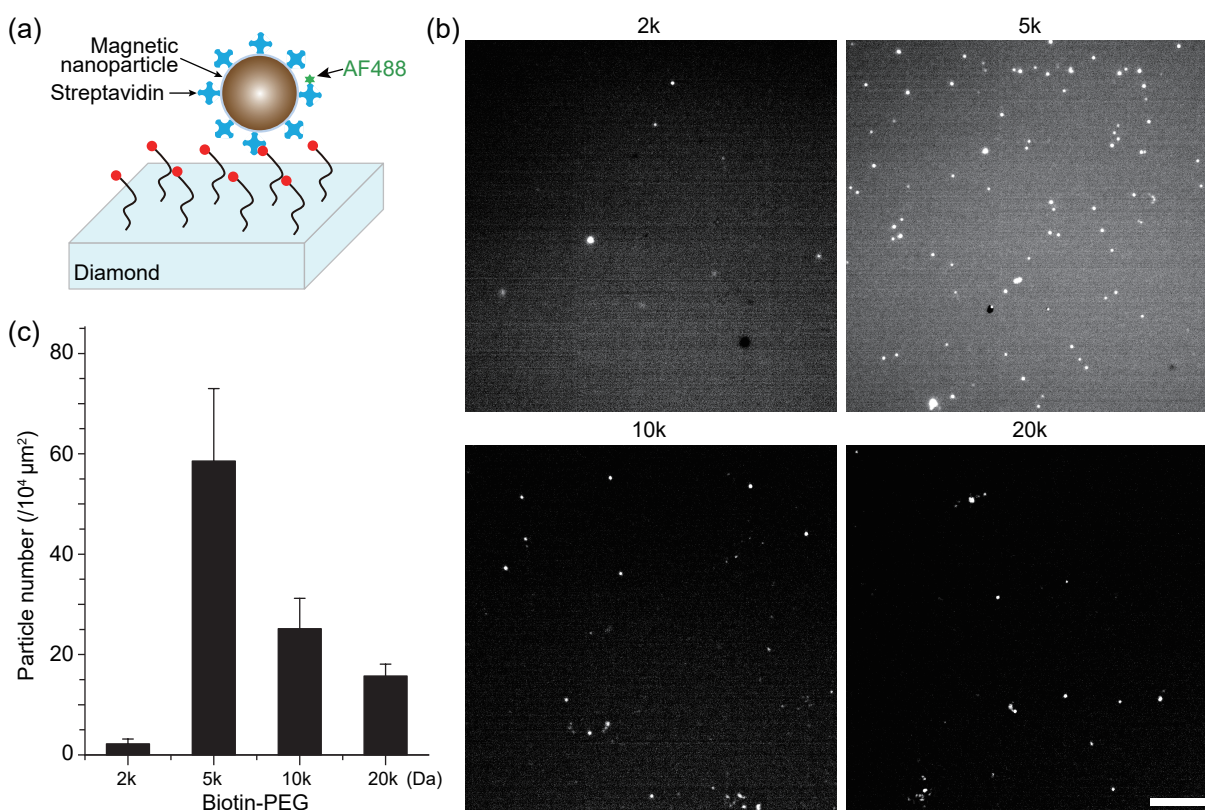


Fig. 3. Binding efficiency of SA-MNPs on diamond surfaces functionalized with biotin-PEG with different MWs. (a) Schematic of the experiment. 100% Biotin-PEG with different MWs was preimmobilized on the diamond, followed by the binding of SA-MNPs via the biotin-SA interaction. The fluorophore Alexa Fluor 488 (AF488) was conjugated to SA for fluorescence examination. (b) Single-particle fluorescence images of AF488-SA-MNPs on diamonds. The MWs of biotin-PEG are indicated in the figure. Scale bar, 10 μm . (c) Quantification of MNP densities in (b). Data are presented as the mean \pm SEM, $n \geq 3$ areas for each group.

diamond quantum sensing of biomolecules, SA connected to biotin-PEG on the sensor serves as a specific binding site of molecules^[11,26]. However, we found that the SA at the end of biotin-PEG affects the elimination of NSB on the diamond surface (Fig. 4). In the examinations, we compared the NSB with SA or without SA in the systems. Antibodies are usually introduced as molecular tools in biomolecular studies and biomolecular assays in clinical diagnosis. Here, we selected the immunoglobulin G (IgG)-coated MNP with AF488 (AF488-IgG-MNP) as a typical biomolecule or nanoparticle to determine the NSB on the diamond surface (Fig. 4). Unexpectedly, as the best overall performance group in the previous section, the passivation of 5 kDa biotin-PEG was severely disrupted by SA. These results suggest that the polymer architecture of 5 kDa biotin-PEG was altered by the bound SA, thereby reducing the passivation effect. However, 20 kDa biotin-PEG steadily eliminated NSB, regardless of the presence of SA. We explain that the 20 kDa biotin-PEG chain is longer, the SA at the end of the chain has less impact, and the PEG polymer still exerts a significant effect on eliminating NSB.

In addition to the use of longer biotin-PEGs to eliminate the impact of SA binding, another straightforward strategy is to dilute the binding sites of SA by mixing biotin-PEG with nonbiotinylated mPEG. Similarly, in single-molecule studies, PEG/biotin-PEG doping is commonly used to prepare single-molecule samples. Next, we evaluated NSB when different ratios of 5 kDa mPEG to biotin-PEG were used (Fig. 5a). We found that the particle density decreased as the proportion of mPEG increased (Fig. 5b, c). NSB was significantly

inhibited when the mPEG-to-biotin-PEG ratio was equal to or greater than 5 : 1. When the mPEG-to-biotin-PEG ratio reached 20 : 1, the MNP density was comparable to that observed in the control group (biotin-PEG-treated diamond without SA).

In summary, the presence of SA interferes with NSB elimination of biotin-PEG on diamond surfaces, reflecting the impact of binding biomolecules at the end of PEG. Nevertheless, this problem can be largely mitigated by using 20 kDa or larger biotin-PEG or a 5 kDa PEG mixture (mPEG : biotin-PEG \geq 5 : 1).

3.4 Biomolecular assay with passivated and functionalized diamonds

Implementing NV center-based highly specific and sensitive quantum sensing of biomolecules is the primary aim of passivating and functionalizing diamond surfaces. As a demonstration, we carried out single-particle immunomagnetic assays (SPIMAs) based on single-particle magnetic imaging (SiPMI)^[11] for antibodies against the receptor-binding domain (RBD) of SARS-CoV-2 spike proteins to assess the efficacy of PEG-based surface modifications (Fig. 6a). Before the SPIMA experiments, we measured NVs' comparable fluorescence intensities and continuous-wave (CW) spectra in the bare diamond and PEGylated diamond (Fig. S2), excluding negative effects from PEG treatments on the diamond magnetic-field sensors. Moreover, the robustness and repeatability of the PEGylation processes were verified by the comparable single-particle fluorescence results of purified anti-RBD-antibody samples on the diamonds in two independent

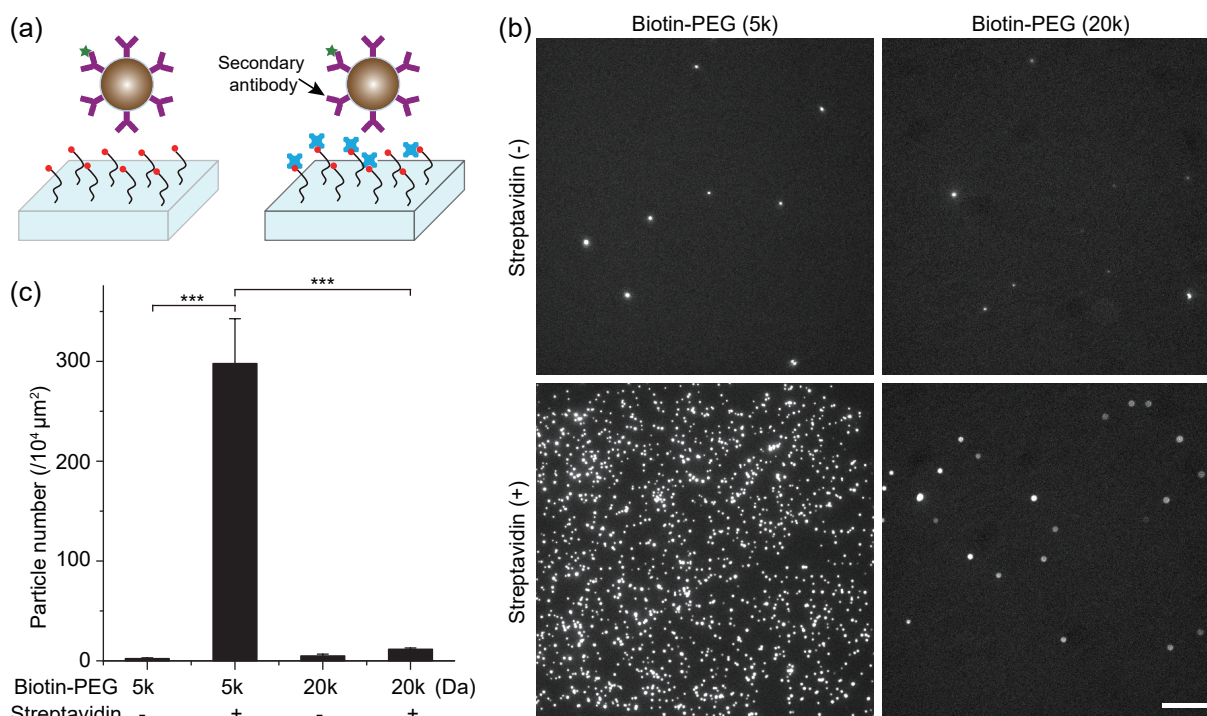


Fig. 4. The NSB of antibody-MNPs on biotin-PEG-functionalized diamonds bound by SA. (a) As shown in the schematic, the antibody-coated MNP was employed to evaluate the extent of NSB on the biotin-PEG-functionalized diamond with SA. The group without SA served as the control. (b) Fluorescence images of AF488-antibody-MNPs on biotin-PEG-functionalized diamonds with SA [streptavidin (+)] or without SA [streptavidin (-)]. The MWs of biotin-PEG were 5 kDa and 20 kDa, respectively. Scale bar, 20 μm. (c) Quantification of MNP densities in (b). Data are presented as the mean \pm SEM, $n \geq 5$ areas for each group. *** $P < 0.001$, t test.

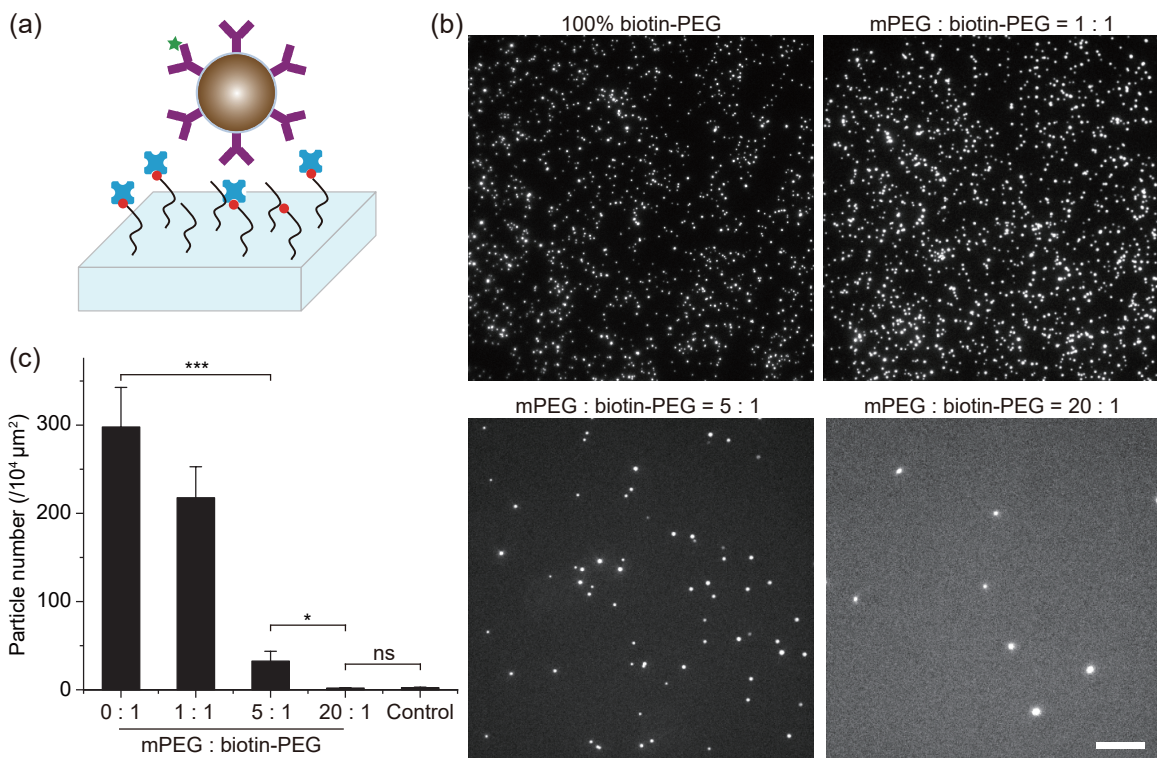


Fig. 5. NSB of antibody-MNPs on diamond treated with a 5 kDa mPEG/biotin-PEG mixture. (a) The schematic shows a diamond surface PEGylated by an mPEG/biotin-PEG mixture, followed by SA binding. (b) Fluorescence images of AF488-antibody-MNPs on diamonds treated by PEG mixtures with different mPEG-to-biotin-PEG ratios. Scale bar, 20 μm. (c) Quantification of MNP densities in (b). Data are presented as the mean ± SEM, $n \geq 5$ areas for each group. * $P < 0.05$, *** $P < 0.001$, ns: not significant ($P > 0.05$), t test.

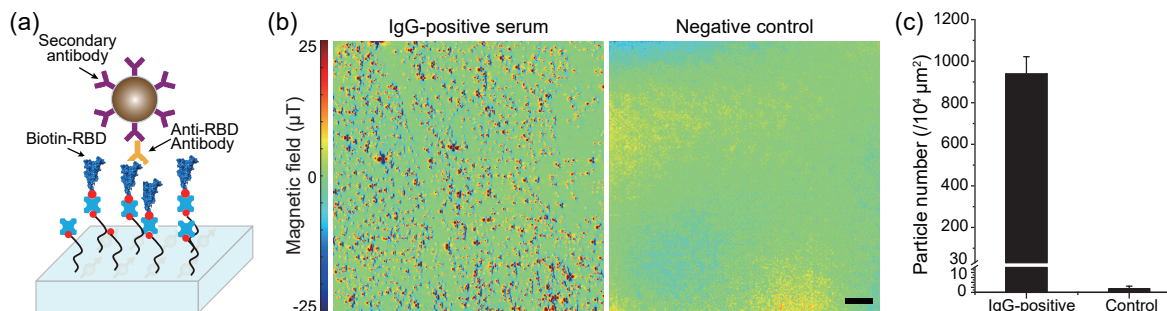


Fig. 6. Single-particle immunomagnetic assays (SPIMAs) of spike RBD antibodies. (a) The diamond surface treated by 20 kDa biotin-PEG is preimmobilized with biotin-RBD proteins. The target molecule, the anti-RBD antibody, is captured via the specific antigen–antibody interaction. Secondary antibody-conjugated MNPs are introduced to identify anti-RBD antibodies. Single MNPs are detected by SiPMI. (b) Single-particle magnetic images of the IgG-positive serum group and the negative control group. The human serum samples were examined without dilution. More details of the serum samples can be found in the Materials and methods section. The magnetic images were denoised via the wavelet threshold denoising method. Scale bar, 10 μm. (c) Quantification of MNP densities in (b). Data are represented as the mean ± SEM, $n \geq 5$ areas for each group.

experiments (Fig. S3). For human serum samples, the SiPMI results showed that SPIMA specifically detected the RBD antibodies (Fig. 6), confirming the specificity of our PEG-based functionalization scheme in real clinical samples. Collectively, these results confirm that PEG-based surface modification is highly specific and compatible with diamond quantum sensing of biomolecules.

4 Conclusions

In this work, we systematically explored PEG treatment conditions on NV-hosted diamond for biomolecular quantum sensing. PEGylation and functionalization were achieved in less than 24 h through routine mild chemical reactions. The

optimal PEG treatments, which involve the use of a 5 kDa PEG mixture with an mPEG-to-biotin-PEG ratio greater than 5 : 1 or pure 20 kDa biotin-PEG, significantly reduce nonspecific binding on the diamonds and allow specific streptavidin-mediated immobilization of the target molecules without degrading the NV sensors. On the diamonds, we can control the distance between biomolecules and even prepare single molecules by adjusting the mPEG-to-biotin-PEG ratio, and control the molecule-NV longitudinal distance by changing the PEG chain length^[35]. The PEG polymer can also be extended as a nanoscale force transducer, integrating mechanical readouts with quantum measurements^[37]. In conclusion, this PEG-based method provides a versatile and biocompatible

platform for efficient and specific quantum sensing of biomolecules, and will provide new opportunities for biomolecular studies and ultrasensitive assays of biomolecules in clinical diagnosis.

In future studies, refined silanization treatments^[38] and plasma treatments^[39], and hydrogel coats^[12] on diamonds can be introduced to improve the functionalization efficiency and scalability. In addition, FRET-driven site-directed modification^[40] could support spatially accurate molecular attachment on diamonds for nanoscale sensing.

Supporting information

The supporting information for this article can be found online at <https://doi.org/10.52396/JUSTC-2025-0047>. The supporting information includes three figures.

Acknowledgements

This work was supported by the National Natural Science Foundation of China (T2125011, 32471527), the National Key R&D Program of China (2021YFB3202800), the CAS (YSBR-068), Innovation Program for Quantum Science and Technology (2021ZD0302200, 2021ZD0303204), New Cornerstone Science Foundation through the XPLOER PRIZE, Hefei Comprehensive National Science Center, the Leading Talents of Innovation and Entrepreneurship of Jiangsu Province (JSSCRC2023548), the Leading Talents of Innovation and Entrepreneurship of Gusu District (ZXL2024351), and the Fundamental Research Funds for the Central Universities. We thank the Biomedical Platform at the Suzhou Institute for Advanced Research of University of Science and Technology of China for providing technical support.

Conflict of interest

The authors declare that they have no conflict of interest.

Biographies

Ziting Sun is a postdoctor at the School of Physical Sciences, University of Science and Technology of China (USTC). He received his Ph.D. degree in Quantum Information Physics from USTC in 2025. His research mainly focuses on biomedical applications of nitrogen-vacancy (NV) centers in diamond.

Sanyou Chen is a Professor at the University of Science and Technology of China. He received his Ph.D. degree in Biophysics from Huazhong University of Science and Technology in 2014. His research mainly focuses on biomedical applications of diamond NV center-based quantum sensing.

Fazhan Shi is a Professor at the University of Science and Technology of China (USTC). He received his Ph.D. degree in Physics from USTC in 2013. His research mainly focuses on spin-based quantum sensing and its applications.

References

[1] Zhang T, Pramanik G, Zhang K, et al. Toward quantitative biosensing with nitrogen-vacancy center in diamond. *ACS Sensors*,

2021, 6: 2077–2107.

- [2] Du J, Shi F, Kong X, et al. Single-molecule scale magnetic resonance spectroscopy using quantum diamond sensors. *Reviews of Modern Physics*, 2024, 96: 025001.
- [3] Aslam N, Zhou H, Urbach E K, et al. Quantum sensors for biomedical applications. *Nature Reviews Physics*, 2023, 5: 157–169.
- [4] Shi F, Zhang Q, Wang P, et al. Single-protein spin resonance spectroscopy under ambient conditions. *Science*, 2015, 347: 1135–1138.
- [5] Shi F, Kong F, Zhao P, et al. Single-DNA electron spin resonance spectroscopy in aqueous solutions. *Nature Methods*, 2018, 15: 697–699.
- [6] Lovchinsky I, Sushkov A O, Urbach E, et al. Nuclear magnetic resonance detection and spectroscopy of single proteins using quantum logic. *Science*, 2016, 351: 836–841.
- [7] Glenn D R, Lee K, Park H, et al. Single-cell magnetic imaging using a quantum diamond microscope. *Nature Methods*, 2015, 12: 736–738.
- [8] Wang P, Chen S, Guo M, et al. Nanoscale magnetic imaging of ferritins in a single cell. *Science Advances*, 2019, 5: eaau8038.
- [9] Chen S, Li W, Zheng X, et al. Immunomagnetic microscopy of tumor tissues using quantum sensors in diamond. *Proceedings of the National Academy of Sciences of the United States of America*, 2022, 119: e2118876119.
- [10] Nie L, Nusantara A C, Damle V G, et al. Quantum monitoring of cellular metabolic activities in single mitochondria. *Science Advances*, 2021, 7: eabf0573.
- [11] Chen S, Sun Z, Li W, et al. Digital magnetic detection of biomolecular interactions with single nanoparticles. *Nano Letters*, 2023, 23: 2636–2643.
- [12] Kayci M, Fan J, Bakirman O, et al. Multiplexed sensing of biomolecules with optically detected magnetic resonance of nitrogen-vacancy centers in diamond. *Proceedings of the National Academy of Sciences of the United States of America*, 2021, 118: e2112664118.
- [13] Miller B S, Bezing L, Gliddon H D, et al. Spin-enhanced nanodiamond biosensing for ultrasensitive diagnostics. *Nature*, 2020, 587: 588–593.
- [14] Naresh V, Lee N. A review on biosensors and recent development of nanostructured materials-enabled biosensors. *Sensors*, 2021, 21: 1109.
- [15] Perillat D, Tan H, Zuk R, et al. Label-free detection of biomolecular interactions using BioLayer interferometry for kinetic characterization. *Combinatorial Chemistry & High Throughput Screening*, 2009, 12: 791–800.
- [16] Nguyen H H, Park J, Kang S, et al. Surface plasmon resonance: A versatile technique for biosensor applications. *Sensors*, 2015, 15: 10481–10510.
- [17] Nie B, Yang M, Fu W, et al. Surface invasive cleavage assay on a maskless light-directed diamond DNA microarray for genome-wide human SNP mapping. *Analyst*, 2015, 140: 4549–4557.
- [18] Szunerits S, Nebel C E, Hamers R J. Surface functionalization and biological applications of CVD diamond. *MRS Bulletin*, 2014, 39: 517–524.
- [19] Yang W, Baker S E, Butler J E, et al. Electrically addressable biomolecular functionalization of conductive nanocrystalline diamond thin films. *Chemistry of Materials*, 2005, 17: 938–940.
- [20] Yang W, Auciello O, Butler J E, et al. DNA-modified nanocrystalline diamond thin-films as stable, biologically active substrates. *Nature Materials*, 2002, 1: 253–257.
- [21] Härtl A, Schmich E, Garrido J A, et al. Protein-modified nanocrystalline diamond thin films for biosensor applications. *Nature Materials*, 2004, 3: 736–742.
- [22] Janitz E, Herb K, Völker L A, et al. Diamond surface engineering for molecular sensing with nitrogen: Vacancy centers. *Journal of Materials Chemistry C*, 2022, 10: 13533–13569.

- [23] Hauf M V, Grotz B, Naydenov B, et al. Chemical control of the charge state of nitrogen-vacancy centers in diamond. *Physical Review B*, **2011**, *83*: 081304.
- [24] Stacey A, Karle T J, McGuinness L P, et al. Depletion of nitrogen-vacancy color centers in diamond via hydrogen passivation. *Applied Physics Letters*, **2012**, *100*: 071902.
- [25] Abendroth J M, Herb K, Janitz E, et al. Single-nitrogen-vacancy NMR of amine-functionalized diamond surfaces. *Nano Letters*, **2022**, *22*: 7294–7303.
- [26] Xie M, Yu X, Rodgers L V H, et al. Biocompatible surface functionalization architecture for a diamond quantum sensor. *Proceedings of the National Academy of Sciences of the United States of America*, **2022**, *119*: e2114186119.
- [27] Rodgers L V H, Nguyen S T, Cox J H, et al. Diamond surface functionalization via visible light-driven C–H activation for nanoscale quantum sensing. *Proceedings of the National Academy of Sciences of the United States of America*, **2024**, *121*: e2316032121.
- [28] Sankaranarayanan S A, Murugappan S, Eswar K, et al. Polyethylene glycol: Structure, properties, and biomedical applications. In: Jayakumar R, Masson M, Deepagan Gopal D V, editors. *Synthetic Polymers in Drug and Biotherapeutics Delivery*. Cambridge, UK: Woodhead Publishing, **2025**: 197–234.
- [29] Jain A, Liu R, Ramani B, et al. Probing cellular protein complexes using single-molecule pull-down. *Nature*, **2011**, *473*: 484–488.
- [30] Jain A, Liu R, Xiang Y K, et al. Single-molecule pull-down for studying protein interactions. *Nature Protocols*, **2012**, *7*: 445–452.
- [31] Chandross S D, Haagsma A C, Lee Y K, et al. Surface passivation for single-molecule protein studies. *Journal of Visualized Experiments*, **2014**, *86*: 50549.
- [32] Chen S, Li L, Li J, et al. SEC-10 and RAB-10 coordinate basolateral recycling of clathrin-independent cargo through endosomal tubules in *Caenorhabditis elegans*. *Proceedings of the National Academy of Sciences of the United States of America*, **2014**, *111*: 15432–15437.
- [33] Upadhyayula S, Quinata T, Bishop S, et al. Coatings of polyethylene glycol for suppressing adhesion between solid microspheres and flat surfaces. *Langmuir*, **2012**, *28*: 5059–5069.
- [34] de Gennes P G. Conformations of polymers attached to an interface. *Macromolecules*, **1980**, *13*: 1069–1075.
- [35] Li M, Jiang S, Simon J, et al. Brush conformation of polyethylene glycol determines the stealth effect of nanocarriers in the low protein adsorption regime. *Nano Letters*, **2021**, *21*: 1591–1598.
- [36] Dundas C M, Demonte D, Park S. Streptavidin–biotin technology: Improvements and innovations in chemical and biological applications. *Applied Microbiology and Biotechnology*, **2013**, *97*: 9343–9353.
- [37] Xu F, Zhang S, Ma L, et al. Quantum-enhanced diamond molecular tension microscopy for quantifying cellular forces. *Science Advances*, **2024**, *10*: eadi5300.
- [38] Antoniou M, Tsounidi D, Petrou P S, et al. Functionalization of silicon dioxide and silicon nitride surfaces with aminosilanes for optical biosensing applications. *Medical Devices & Sensors*, **2020**, *3*: e10072.
- [39] McCloskey D J, Roberts D, Rodgers L V H, et al. Methods for color center preserving hydrogen-termination of diamond. *Advanced Materials Interfaces*, **2024**, *11*: 2400242.
- [40] Goun A, Rabitz H A. Co-localization of surface-bound molecules and shallow luminescent centers utilizing Forster resonant excitation transfer driven photochemical reactions. In: *Proceedings Volume 12863, Quantum Effects and Measurement Techniques in Biology and Biophotonics*. San Francisco, CA, USA: SPIE, **2024**: 128630A.